Viral Mimicry and its Impact on Cell Biology: Investigations into the Roles of Epstein-Barr Virus (EBV) Latent Membrane Proteins LMP1 and LMP2a

A Senior Thesis Presented to
The Faculty of the Department of Molecular and Cellular Biology,
Colorado College

By
Nora Watkins
Bachelor of Arts Degree in Molecular and Cellular Biology
Submitted April 26, 2019

Dr. Olivia Hatton
Primary Thesis Advisor

Dr. Phoebe Lostroh
Secondary Thesis Advisor

Abstract

Epstein-Barr Virus (EBV)-associated cancers including post-transplant lymphoproliferative disorder (PTLD) and Burkitt's lymphoma account for close to 2% of global cancer deaths annually. Two EBV proteins, latent membrane proteins 1 and 2a (LMP1 and 2a) are of interest for their roles in latent infection and cancer formation. LMP1 is a functional mimic of the native B cell receptor protein CD40 and drives proliferation in infected cells. In the native context, B cells require two signals to undergo activation: one from the B cell receptor (BCR) and a second signal from either CD40 or TLR9. Without a second signal, B cells will experience mitochondrial dysfunction eventually leading to apoptosis in a phenomenon known as activation-induced cell death (AICD). We sought to determine if signaling from LMP1 would be able to "rescue" two Burkitt's lymphoma cell lines expressing a chimeric LMP1 protein (NGFR.LMP1) from AICD. We were unable to determine conclusively whether signaling from NGFR.LMP1 was able to rescue cells from AICD but data indicate a potential trend for LMP1's ability to inhibit AICD in human LCLs. Further investigation into the functional similarities between CD40 and LMP1 are required to understand the biology of EBV-infected cells and associated cancers.

LMP2a is an EBV protein present in the membrane of infected human B cells and implicated in establishing and maintaining EBV^+ B cell cancers. We aimed to generate EBV^- B cell lines that stably express a chimeric LMP2a molecule that permits induction of LMP2a signaling; these lines will be used to examine how LMP2a alters infected-cell biology and drives EBV^+ B cell cancers. Initially, optimal DNA transfection and selection media conditions for both EBV^- B cell lines were determined. DNA for the chimeric Ly49G.LMP2a protein was synthesized in a bacterial expression vector and *E. coli* were transformed. Ly49G.LMP2a DNA was isolated from bacterial plasmid DNA by restriction enzyme digestion, purified, and subsequently ligated into a mammalian expression vector. Using Sanger sequencing and restriction enzyme digests, we confirmed successful cloning of Ly49G.LMP2 into the expression vector. These vectors were

then transfected into two EBV^- B cell lines. By creating these cell lines, we aim to determine the role of LMP2a in the development and biology of EBV^+ B cell cancers.

Introduction

Epstein-Barr Virus (EBV) is a gamma herpesvirus that exists as a latent infection in up to 95% of human adults (Figure 1). A wide range of clinical outcomes are associated with viral infection and depend greatly on factors including age during primary infection and immune system status. If primary infection occurs in childhood, illness typically presents as a subclinical upper respiratory tract infection. In adolescence, the virus can cause infectious mononucleosis, known as "mono." EBV infection is also strongly associated with a number of cancers, including post-transplant lymphoproliferative disorder (PTLD), Burkitt lymphoma, and Hodgkin's disease[1] and recently, research has begun investigating EBV's association with multiple sclerosis (MS)[2]. The extreme variation in clinical outcomes associated with EBV infection are indicative of a complex network of interactions between virus and host.

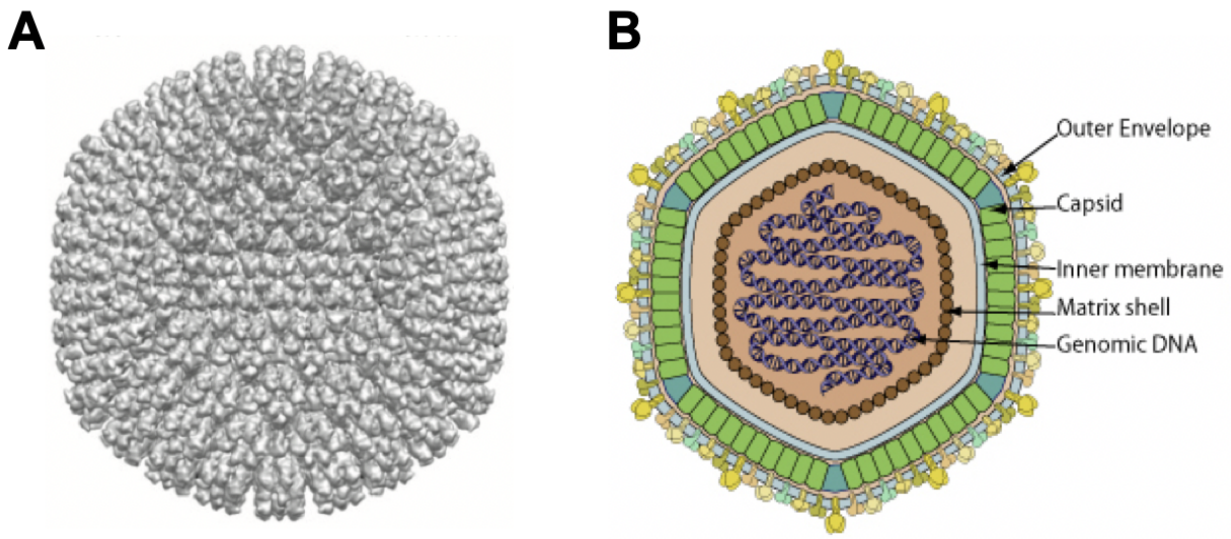

Figure 1. Epstein-Barr Virus. a) Computer-generated rendering of outer capsid of the virus from electron microscope images. b) Schematic of viral structure.

Following primary lytic infection of either pharyngeal epithelial or naive B cells, EBV is able to persist as a latent infection for the lifetime of the host in memory B cells[1]. Three distinct patterns

of latent infection are characterized by different patterns of viral gene expression. Many EBV$^+$ cancers are associated with latency pattern III which is characterized by co-expression of Epstein-Barr nuclear antigen (EBNA)-1, EBNA-2, EBNA-3A-C, EBNA-LP, latent membrane protein 1 (LMP1), and LMP2a[3]. Latency III is the most immunogenic form of latency owing to the high number of viral proteins expressed and is thus commonly associated with diseases affecting immunocompromised or immunosuppressed patients[4].

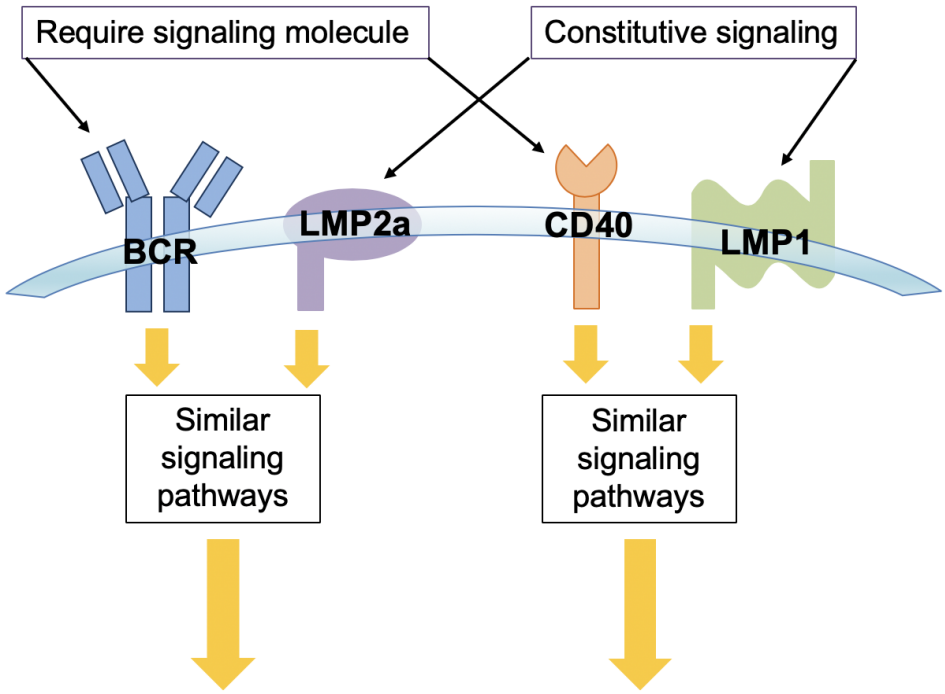

Figure 2. Comparison of native B cell proteins and their EBV mimics. The B-cell receptor (BCR) and CD40 are native B cell proteins involved in B cell activation. They require the binding of ligand in order to signal. LMP1 and LMP2a are EBV mimic proteins that mimic the signaling activity of CD40 and BCR, respectively. They are constitutively active.

Several EBV proteins are functional mimics of native B cell proteins and utilize similar signaling pathways to alter normal B cell function (Figure 2). LMP1 is a viral mimic of the B cell costimulatory molecule CD40[5,6]. Unlike CD40, which only signals when triggered by the presentation of CD40L from helper T cells, LMP1 exhibits constitutive activity and activates NF-κB, API, and ATF2, which inhibit apoptosis[4]. LMP1 is also known to drive the formation of transformed lymphoblastoid cell lines (LCLs) *in vitro*[3] and enhances the formation of lymphoid

tumors in an *in vivo* mouse model[4]. A non-constitutively active chimeric version of LMP1 has been demonstrated to be able to functionally replace CD40 in a transgenic mouse model[7]. LMP2a is a constitutively active viral mimic of the B cell receptor (BCR)[7,8], which in the native context is only activated by binding of antigen. It has been demonstrated to promote survival of peripheral B cells[4] but is not required for transformation of naive B cells into LCLs[7]. Importantly for latent infection, LMP2a has been demonstrated to allow infected cells to undergo the germinal center (GC) reaction which results in differentiation into memory cells. LMP1 allows for cytokine independent class-switch recombination (CSR). Together, LMP1 and LMP2a commit infected B cells toward terminal differentiation resulting in the formation of memory B cells containing the EBV genome[7].

Recently the role that metabolic activity, specifically that of mitochondria, plays in determinations of cell fate has begun to come to light. B cells have different metabolic profiles depending on their state of activation. When stimulated with lipopolysaccharide (LPS), an endotoxin produced by gram-negative bacteria that triggers an inflammatory immune response, or via the BCR, normal B cells exhibit signs of heightened metabolic activity including increased lactate production and rate of oxygen consumption (OCR) in conjunction with increases in mitochondrial mass[9]. By contrast, quiescence in B cells is maintained by the interplay of signals from BCR and B cell activating factor receptor (BAFFR) and is reliant on the maintenance of a balance of mitochondrial synthesis and clearance[10,11]. B cell activity, generally, is highly dependent on the ability for cells to undergo rapid metabolic changes. Following activation, B cells exit G_0 and enter a period of growth before entering S phase characterized by increased energetic and macromolecule synthetic demands[12]. Clonal expansion requires the availability of many metabolic products and precursors which necessitates increased glucose and glutamine uptake[12,13] and during clonal expansion, a PI3K-dependent signal transduction cascade upregulates the active glucose transporter GLUT1[9,12]. The process of clonal expansion involves many simultaneous processes and a high degree of coordination of metabolic activity[10]. The

cellular metabolic requirements of proper B cell activation are highly regulated and involved the interplay of many different cellular systems including metabolism.

Proper B cell activation also requires the presence of mitochondrial reactive oxygen species (mROS) downstream of BCR stimulation. mROS production occurs in two waves following BCR stimulation, the first of which is immediate and induced by activation of signaling pathways downstream of *Nox2* (NADPH oxidase isoform present in B cells) and is dispensable for B cell activation. The second and more prolonged wave of resultant mROS production likely derives from increased mitochondrial activity and is essential for activation. Without prolonged ROS production, signals for increased cellular metabolism, growth, and energy uptake through PI3K-related pathways are severely attenuated leading to impaired activation and proliferation[14]. ROS signaling has also been found to play an early role in cell-fate determination in B cells demonstrated by the ability of B cell fate to be predicted by pre-differentiation metabolic profiles[15] and that attenuation of ROS production by glycogen synthase kinase 3 (GSK3) restrains growth in resting B cells[16]. Ahead of ROS signaling and its associated pathways, B cells require two temporally distinct signals in order to undergo proper activation. If these do not occur in the proper sequence and timeframe, mitochondrial injury and ultimately cell death occur. The first signal comes from the BCR when it is stimulated with antigen. There is then a crucial window of time (~9 hours) in which a second signal must be received. This second signal can come via CD40 from presentation of CD40L by a helper T cell or detection of CpG DNA by toll-like receptor (TLR)-9. After the second signal, activation-related metabolic changes begin. Rates of oxidative phosphorylation, glycolysis, and mitochondrial mass increase in preparation for the subsequent metabolic demands of proliferation.

In contrast, If BCR stimulation occurs without co-stimulation by CD40 or CpG, these changes will not occur and instead, signs of mitochondrial stress and dysfunction increase, coinciding with increased ROS and intracellular calcium[17]. Although presence of increased ROS is associated with mitochondrial dysfunction, mitigation of ROS activity with antioxidants did not

decrease mitochondrial injury while the addition of a calcium chelating agent was able to decrease mitochondrial dysfunction. Accordingly, mitigation of ROS activity with antioxidants did not block mitochondrial dysfunction. These findings indicate that mitochondrial injury following BCR stimulation is caused by inability of the cell to clear excess calcium as it gradually builds within the cell. It has been postulated that the gradual increase in calcium concentration after BCR stimulation acts as a "death clock", giving the cell a specific time frame in which AICD can be blocked by the receipt of a second signal which prevents wasting of resources by improperly activated B cells[18]. The second signal during a normal immune response is provided by the CD40 when the B cell interacts with a helper T cell or CpG (Figure 3).

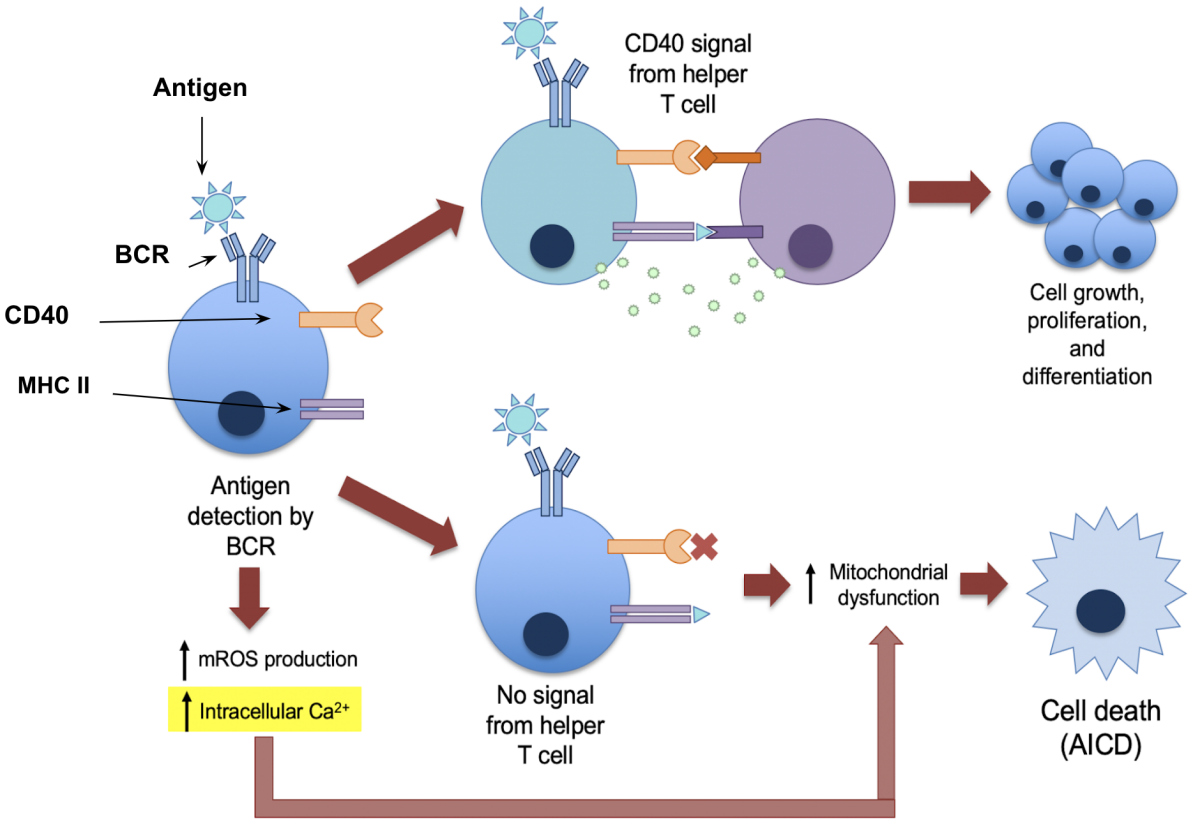

Figure 3. Model of B cell activation-induced cell death (AICD) proposed by Akkaya, et al. 2018. Following antigen detection by the BCR, intracellular mROS and Ca^{2+} increase steadily resulting in two potential cell fates. Either the cell receives a second signal (from either CD40 or TLR9) which attenuates mROS an Ca^{2+} production and results in cell growth, proliferation, and differentiation or increasing levels of these two products result in mitochondrial dysfunction, eventually leading to cell death by apoptosis.

After EBV has infected a B cell, it must avoid AICD despite signaling from the viral BCR mimic LMP2a. The viral protein that most likely fills this role is LMP1 because it is a CD40 mimic. However, some aspects of LMP1 signaling are not completely understood. Although LMP1 has been shown to be able to replace CD40 function in a humanized mouse model, there are differences in the signaling affinities and function between the two proteins. CD40 and LMP1 utilize different TNF receptor associated factors (TRAFs)[7] in downstream signaling and LMP1 is able to induce class-switch recombination (CSR), a process of B cell maturation, independent of cytokine, allowing infected cells to differentiate without the presence of helper T cells[6]. In attempting to better understand EBV and its impact on B cell biology we aimed to determine whether LMP1 signaling could provide a signal similar enough to CD40 to prevent AICD following BCR stimulation. Based on measures of cell proliferation and viability in Ramos Burkitt Lymphoma cells expressing a chimeric NGFR.LMP1, LMP1 signaling demonstrated some ability to provide a rescue effect from AICD however, more trials will be needed to conclusively determine these results. Additionally, we were unable to confirm the ability of native CD40 to provide a rescue but preliminary results suggest that it can.

As a means of further investigating EBV mimics of native B cell proteins, an effort has been made to develop an inducible, chimeric LMP2a that will allow for observation of the effects of LMP2a on B cell function and metabolic activity. A plasmid containing the construct has been developed and will eventually be transfected into BL cell lines for investigation.

Methods

Part I: Effects of LMP1 as a Second Signal on Cell Proliferation and Viability in B cells

Stimulation of Ramos NGFR.LMP1 cells

16 x 10^6 cells were collected from Ramos NGFR.LMP1 A4 and C3 clones in separate 15 mL conical tubes. Cells were centrifuged at 1250 rpm for 5 min, RT and resuspended in cRPMI without G418 to a final concentration of 1 x 10^6 cells/mL. 490µL of cells were distributed into 24-well plates. For samples that were to be stimulated via NGFR.LMP1 cross-linking, mouse anti-human NGFR (BioLegend, Clone ME20.4) was added to a final concentration of 1.02 µg/mL. All samples were then incubated at RT for 30 minutes. cRPMI was added to unstimulated samples to a final concentration of 0.5 x 10^6 cells/mL. For samples stimulated with IgM only, cRPMI with F(ab')2 anti-human IgM + IgG (Bioscience) was added to a final concentration of 5 µg/ 1 x 10^6 cells. For samples stimulated with MEGACD40L only, cRPMI with MEGACD40L (Enzo Life Sciences) was added to a final concentration of 50 ng/ 1 x 10^6 cells. For samples stimulated with NGFR.LMP1 crosslinking only, cRPMI containing goat anti-mouse IgG (Jackson ImmunoResearch) to a final concentration of 8 µg/1 x 10^6 cells. For samples stimulated with both anti-IgM and CD40, cRPMI containing F(ab')2 anti-human IgM + IgG and MEGACD40L was added to final concentrations of 5 µg / 1 x 10^6 cells and 50 ng/ 1 x 10^6 cells, respectively. For samples stimulated with both NGFR.LMP1 cross-linking and anti-IgM, cRMPI containing F(ab')2 anti-human IgM + IgG and goat anti-mouse IgG was added to final concentrations of 5 µg/ 1 x 10^6 cells and 8 µg/ 1 x10^6 cells, respectively. All samples had a total volume of 980 µL. Following addition of stimulations, cells were incubated at 35 C, 5% CO_2 for either 24 or 48 hours before assessment of proliferation and viability.

Assessing cell proliferation after stimulation

At 24 and 48 h, individual samples were mixed thoroughly in their wells by pipetting and 10.5 µL samples were collected and diluted 1:4 in Trypan blue stain. The concentration of live cells was determined by counting using a hemocytometer.

Assessing cell viability after stimulation

At 24 and 48 h, samples were removed from the 24-well plates and placed into FACS tubes. All samples containing anti-mouse crosslinking antibody were incubated with 1 µL ChromePure Mouse IgG (Jackson ImmunoResearch) and incubated for 15 minutes RT. Samples were centrifuged at 1250 rpm for 5 min at RT. Media was decanted and 1 mL cold FACS buffer (what is the recipe for FACS buffer that we use?) was added. After vortexing, samples were centrifuged at 1250 rpm for 5 min, RT. Supernatant was decanted and cells were resuspended in 100 µL cold FACS buffer and were incubated with PE Mouse anti-ICAM clone HA58 at a final concentration of 20 µg/uL on ice in the dark for 30 minutes. Cells were then washed with 1 mL cold FACS buffer, centrifuged at 1250 rpm for 5 min RT. Supernatant was discarded and cells were resuspended in 400 µL cold FACS buffer. 5 µL of 7-AAD viability stain 50 µg/mLwere added to each sample, vortexed, and incubated on ice until collection with MACSQuant.

Part II: Cloning, Transfection Optimization, and Transfection of Ly49G.LMP2a

Kill Curves

10 million cells from Ramos and BL41 cell lines were isolated from culture flasks and centrifuged at 1250 rpm for 5 minutes and original cRPMI media was removed. Cells were resuspended in cRPMI to a concentration of 1 x 10^6 cells/mL (2X final). 500 µL of cells were aliquotted into 24-well plates and were subsequently diluted with 500 µL cRMPI + hygromycin (stock concentration: 50 mg/mL) or Zeocin (stock concentration 100 mg/mL) to final concentrations of 400, 200, 100, 50, 25, and 0 µg/mL for both hygromycin and Zeocin in both

BL41 and Ramos cell lines. Cells were counted with Trypan blue exclusion at 48 h, 72 h, and 96 h to determine rates of proliferation compared to untreated samples. At 48 h, 500 µL of the cRPMI containing the appropriate concentrations of drug was added to the wells designated for collection at 72 h and 96 h. Cells were prepared as previously described and were diluted with cRPMI + Zeocin to final concentrations of 550, 500, 450, 400, 350, and 0 µg/mL for Ramos cells and 300, 250, 200, 150, 100, and 0 µg/mL for BL41. Cells were counted at 48 h, 72 h, and 96 h with an additional 500 µL of drug-containing media added to 72 h and 96 h wells at 48h.

Transfection Optimization

15 million cells were collected from BL41 and Ramos culture flasks, spun down for 5 minutes, RT, at 1250 rpm and resuspended in serum-free RPMI to a concentration of 7.5 x 10^6 cells/mL and centrifuged at 1250 rpm for 5 minutes. Cells were resuspended in serum-free RPMI to a concentration of 25 x 10^6 cells/mL and pMax GFP plasmid DNA was added to each cell line to a final concentration of 1 µg/ 1 x 10^6 cells. 210 µL of cells were then added to 0.4 um chamber electroporation cuvettes (BioRad). Cells were incubated for 5 minutes at RT and subsequently shocked once using a BioRad Micropulser at 750, 1000, and 1250V. When samples were shocked at 1250V, an “arc” error was given by the Micropulser and a shock was not delivered. Cells were incubated for 10 minutes and subsequently transferred to T25 tissue culture flasks in cRPMI to a final volume of 6.0 mL. To determine the effects of plasmid concentration on transfection efficiency, cells were prepared as described above but all samples were shocked at 1000V with 0.2, 0.5, and 1.0 µg/ 1 x 10^6 cells. To determine the effects of number of shocks on transfection efficiency, cells were prepared as described above but were shocked in the presence of 1 µg/ 1 x 10^6 cells plasmid DNA at 1000V 1, 2 or 3 times. Cells were incubated at 35C, 5% CO_2 for 24 hours before collection for flow-cytometric analysis of viability and GFP-expression. At 24 and 48 h, 2 mL of cells was collected from each of the flasks corresponding to the different transfection conditions and 1 mL were transferred to 2 1.5 mL microcentrifuge tubes. Samples

were centrifuged at 1250 rpm for 5 min, RT, and media was removed. Cells were washed twice with 1 mL cold FACS buffer, spun at 1250 rpm for 5 min, RT. Cells were then resuspended in 200 µL FACS buffer and 7-AAD viability stain was added to a final concentration of 1.25 µg/uL. Cells were briefly vortexed and incubated for 5 minutes at RT before analysis with Guava EasyCyte on 509 nm for detection of GFP and 647 nm for detection of 7-AAD staining.

Construction and sequencing of pcDNA 3.1 Zeo (+) Ly49G.LMP2a plasmid

The desired Ly49G.LMP2a insert containing the cytoplasmic region (aa 1-123) of LMP2a linked to the transmembrane and extracellular regions of the mouse type II signal anchor membrane protein (aa 45-280) Ly49G was synthesized in pUCIDT (Kan) plasmid by IDT Custom Gene Synthesis Services. The appropriate mammalian expression vector, pcDNA3.1 Zeo (+), along with pUCIDT Ly49G.LMP2a were digested with the restriction enzymes XhoI and KpnI HF (NEB) in CutSmart buffer according to the manufacturer's protocol. Fragments from the restriction enzyme digest were then separated via gel electrophoresis. The Ly49G.LMP2a insert and pcDNA3.1 Zeo (+) expression vector were purified from the resulting gel using an NEB Monarch DNA Gel Extraction kit according to the manufacturer's instructions. The purified fragments were then ligated with T4 ligase (Invitrogen) and 5 µL of the reaction product was immediately transformed into competent cells via heat shock. Transformed cells were plated on ampicillin agar plates and grown overnight at 35C. 10 colonies were then selected from the plate and were grown in ampicillin LB overnight. Plasmid DNA was isolated using Qiagen Miniprep kit according to the manufacturer's instructions and was digested with restriction enzymes as described above. The products of the restriction enzyme digest were visualized using gel electrophoresis on a 1% w/v agarose gel with 1X GelRed stain. DNA from each of the 10 colonies selected was sent for Sanger sequencing analysis to confirm the orientation and sequence of the Ly49G.LMP2a insert was correct. The forward primer for sequencing was *T7 Forward:* 5'- TAA TAC GAC TCA CTA TAG

GG -3', the reverse was *BghRev*: 5'- AAC TAG AAG GCA CAG TCG AGG C -3'. Returned sequence trace files were analyzed using Sequencher 5.4.6 software.

Construction and sequencing of pcDNA3.1 Ly49G.LMP2a plasmid

Competent cells were transformed with 500 pg pcDNA3.1 (+) plasmid by heat shock and were grown overnight on a 1X ampicillin (100 µg/mL) agar selection plate at 37C. Two colonies were then selected and grown in 1X LB ampicillin for ~16 h before collection for plasmid DNA extraction. pcDNA3.1 (+) DNA was purified from the LB cultures using Qiagen Plasmid Mini-prep kit according to the manufacturer's instructions. 1.0 µg of pcDNA3.1 (+) and 2.0 µg of pUCIDT Ly49G.LMP2a were then digested in NEBuffer 1 with 1X BSA with XhoI and KpnI enzymes. Reaction products were then separated using gel electrophoresis on a 1% w/v agarose gel with 1X SYBRSafe DNA Stain (ThermoFisher) against GoldBio 1kb ladder. The Ly49G.LMP2a insert and pcDNA3.1 (+) fragments were excised from the gel and purified using a NEB Monarch Gel Purification kit. The resulting DNA fragments were then ligated using NEB T4 DNA Ligation kit and 5 µL of the product was then transformed in competent cells with heat shock. Transformed cells were plated on a 1X ampicillin agar selection plate and grown at 35C overnight. Six colonies were then selected randomly from the plate and were grown in 1X ampicillin LB for ~16 hours before collection for plasmid DNA extraction using Qiagen Mini-prep kit. 5 of the 6 colonies purified yielded plasmid DNA and concentrations and purity were measured by NanoDrop.

Transfection of BL41 and Ramos cells with pcDNA3.1 Zeo (+) Ly49G.LMP2a plasmid

15 x 10^6 cells from both BL41 and Ramos cells lines were isolated from tissue culture flasks and were centrifuged at 1250 rpm for 5 min, RT. Culture media was removed and cells were resuspended in 2 mL serum-free RPMI and were centrifuged at 1250 rpm for 5 min, RT. Media was removed and cells were resuspended in serum-free RPMI to a concentration of 25 x 10^6 cells/mL. 1 µg/1 x 10^6 cells of pcDNA3.1 Zeo (+) Ly49G.LMP2a plasmid DNA from three of

the colonies confirmed to have the appropriate sequence and orientation of the plasmid. 210 µL of cells were transferred to 0.4 nm chamber electroporation cuvettes and incubated at RT for five minutes. Samples were shocked at 1000V once and then allowed to incubate for 10 minutes at RT before being transferred to T25 tissue-culture flasks with cRPMI for a total volume of 6.0 mL. Cells were then placed in a humidified incubator at 35C, 5% CO_2 for 24 hours. Cells were then counted using Trypan blue staining with a hemocytometer and diluted in cRPMI containing the appropriate concentrations of Zeocin for each cell line (150 µg/mL for BL41, 450 µg/mL for Ramos) to 100 cells/mL, and 1000 cells/mL for BL41 and 1000 cells/mL and 10000 cells/mL for Ramos. Dilutions were plated in 96-well plates and incubated at 35C, 5% CO_2 and were checked weekly for clones.

Results

Part I: Effects LMP1 as a Second Signal on Cell Proliferation and Viability in B cells

Functionality of NGFR.LMP1 construct is confirmed by increased ICAM expression

The EBV CD40 mimic LMP1 is constitutively active in EBV-infected cells. To better isolate its cellular effects, Ramos cells expressing an inducible version of LMP1, NGFR.LMP1, created using the transfection optimization data described above were stimulated with either CD40L or with crosslinking of NGFR.LMP1 which causes the construct to aggregate in the cell membrane and signal. Signaling from native CD40 results in increased expression of CD54, or intercellular adhesion molecule 1 (ICAM-1). Upregulation of ICAM-1 can be used as an indicator for signaling by CD40 or the viral mimic LMP1. To demonstrate the functionality of the NGFR.LMP1 construct system, cells were stimulated for either 24 or 48 hours with NGFR-crosslinking or CD40L and ICAM expression was quantified by flow cytometry compared to unstimulated cells. Consistently, cells stimulated with NGFR.LMP1 crosslinking or CD40L exhibited increased ICAM expression compared with unstimulated cells. Representative data is shown in Figure 4. Median fluorescent intensity (MFI) increased 3.09 fold in A4 cells and 2.85 fold in C3 cells after NGFR.LMP1 crosslinking. MFI increased 3.34 fold in A4 cells and 2.61 fold in C3 cells after stimulation with CD40L. The similarity in magnitude of increases in fold-change expression of ICAM between the two stimulation conditions indicate CD40 and LMP1 had similar cellular effects and demonstrates the functionality of the NGFR.LMP1 construct.

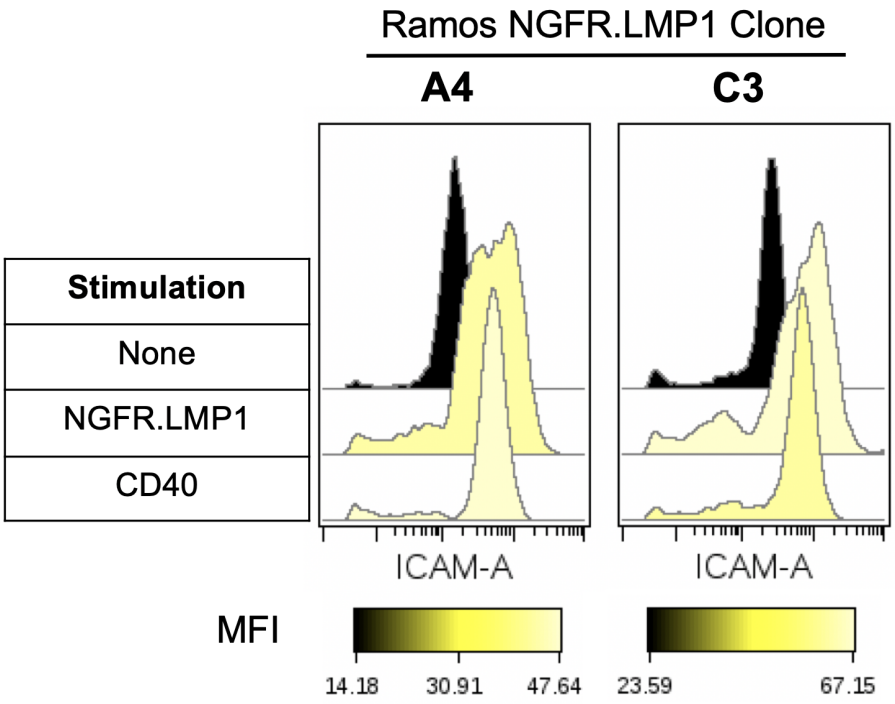

Figure 4. Stimulation of Ramos NGFR.LMP1 B cells via CD40 and NGFR.LMP1 increases ICAM expression. Ramos NGFR.LMP1 cells were stimulated for 24 or 48 hours with NGFR.LMP1 crosslinking or MEGACD40L before analysis of ICAM expression with flow cytometric staining for surface ICAM. Median fluorescence intensity (MFI) is expressed as a gradient from black to yellow.

NGFR.LMP1 crosslinking increases MitoTracker Green staining at 48 h

Previously, stimulation of Ramos cells with CD40L has resulted in increased staining with MitoTracker Green (data not shown) which can be used as a measure of mitochondrial mass. In order to determine if a similar effect can be seen with NGFR.LMP1 crosslinking, cells were stimulated for 48 hours with crosslinking. In two of three newly generated Ramos NGFR.LMP1 clones (A2, A4, and C3) stimulation of cells with NGFR.LMP1 crosslinking resulted in significantly increased MitoTracker Green staining (Figure 5a) which suggests an increase in mitochondrial mass. A2 cells experienced an average of 1.5-fold increase, while A4 and C3 cells had a 1.4 and 2.0 fold increase, respectively. In comparisons between pooled data from all three clones,

differences in MitoTracker Green staining between stimulated and unstimulated cells were found to be significant ($p < .05$) with an average fold change of 1.6 (Figure 5b).

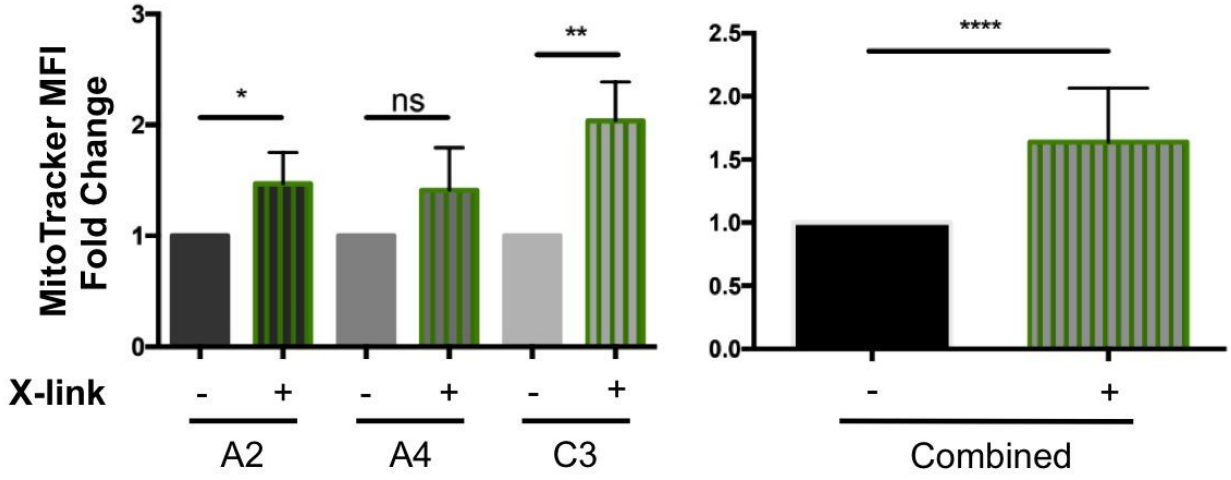

Figure 5. NGFR.LMP1 significantly increases mitochondrial mass in two Ramos NGFR.LMP1 clones (left) and on average for all three clones (right). Ramos NGFR.LMP1 cells were stimulated for 48 h with 2 µg/ 1 x 10^6 cells mouse anti-human NGFR and 2 µg/ 1 x 10^6 cells goat anti-mouse cross-linking antibody before collection for analysis via flow cytometry. Cells were then stained with MitoTracker Green to a final concentration of 100 nM and 7-AAD. Amount of MitoTracker Green staining correlates to mitochondrial mass in cells. Fold change in ICAM expression was determined by normalizing MitoTracker Green MFI of stimulated samples to unstimulated controls for each cell line.

Signaling from CD40 or NGFR.LMP1 may be able to rescue cells from AICD

As NGFR.LMP1 has been demonstrated to be functionally similar to CD40 in its ability to affect cellular biology in a way that leads to increased mitochondrial staining, investigations into other functional similarities between the two proteins are relevant. CD40 signaling has been demonstrated in an *in vivo* model to be able to rescue cells stimulated via the BCR from activation-induced cell death (AICD). Ramos NGFR.LMP1 clones A4 and C3 were stimulated via the BCR, NGFR.LMP1, CD40 alone, or by a combination of BCR and NGFR.LMP1 or BCR and CD40 in order to determine the effects of signaling on cell proliferation and viability. Trials in which BCR stimulation alone did not induce cell death or viability above 50% were excluded from analysis. There was a substantial difference in cell proliferation in both cell lines at 24 and 48 hours between

cells stimulated with BCR alone and BCR+CD40 with greater proliferation in cells stimulated with both BCR and CD40. For example, average proliferation compared to unstimulated in A4 cells stimulated with BCR alone at 24 h was 32.9% while stimulation with BCR+CD40 resulted in 67.9% proliferation. Proliferation in C3 cells at 48 h with BCR stimulation alone was 10.4% but with CD40 in addition to BCR, proliferation was 90.5% of unstimulated. These data suggest CD40 is able to provide a sufficient second signal to rescue B cells from AICD induced by BCR stimulation.

BCR costimulation with the NGFR.LMP1 construct provided a less substantial and less consistent rescue effect. For example, A4 cells at 24 hours stimulated with BCR alone had 32.9% proliferation compared to unstimulated while cells stimulated with BCR and NGFR.LMP1 had only 36.6% proliferation. A similar effect size is seen in A4 cells at 48 hours with with BCR-stimulated cells at 14.1% proliferation compared to unstimulated and cells costimulated with NGFR.LMP1 had only 21.6% proliferation. In C3 cells, a larger effect was seen at 48 hours. Cells stimulated with BCR alone had 10.5% proliferation compared to unstimulated while cells costimulated with NGFR.LMP1 had 45.6% proliferation (Figure 6). These results do not provide strong support for NGFR.LMP1's ability to provide a sufficient second signal to rescue cells from AICD but further trials may be required in order to see an effect due to the apparent toxicity of the NGFR.LMP1 construct's activity.

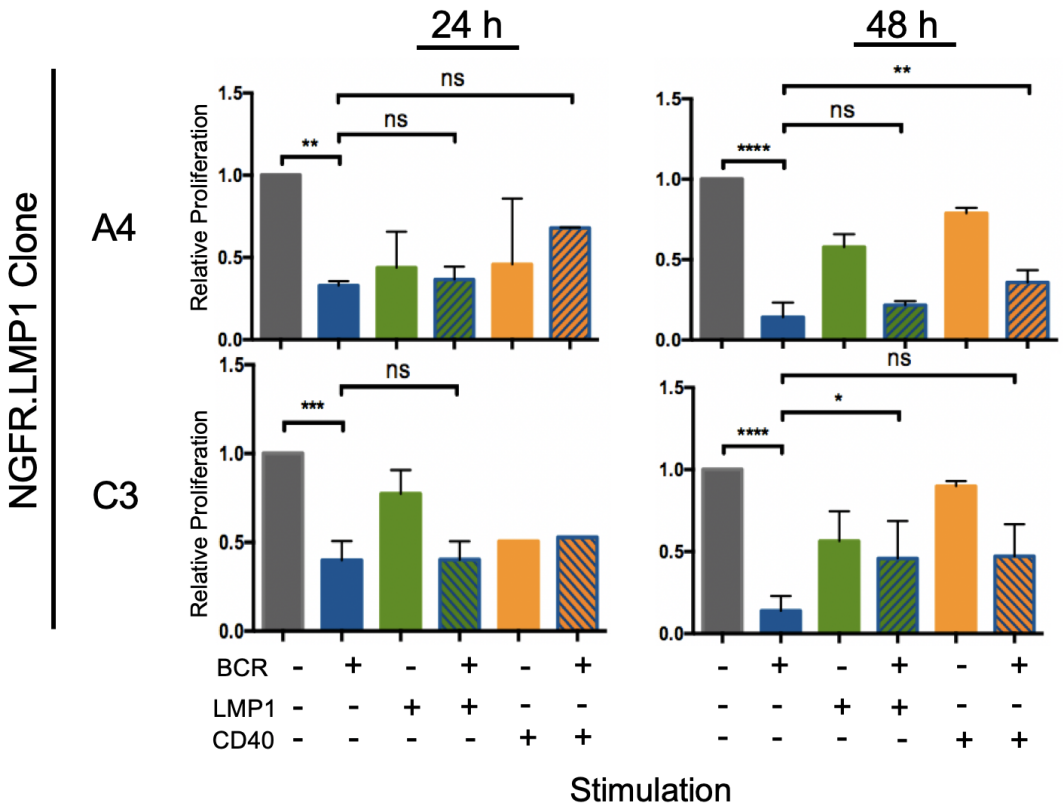

Figure 6. LMP1 and CD40 potentially rescue cells from AICD based on relative proliferation. Two unique clones of Ramos NGFR.LMP1 cells were treated with different stimulations in order to determine the effects of a second signal from either CD40 or NGFR.LMP1. Concentrations of live cells were determined at 24 and 48 h post-stimulation using Trypan blue exclusion. Concentrations of treated cells were normalized to concentrations of unstimulated cells as a measure of cell proliferation. n.s. $p > 0.05$, * $p \leq 0.05$, ** $p \leq 0.01$, *** $p \leq 0.001$, **** $p \leq 0.0001$. One-way ANOVA.

We assessed changes in cell viability under different stimulation conditions using flow cytometry with 7-AAD. In A4 cells at 24 hours, viability of cells stimulated with NGFR and BCR was 36.7% compared to 37.3% for BCR alone but at 48 hours in A4 cells, cells stimulated with BCR and NGFR.LMP1 were 51.1% viable compared to those stimulated with BCR alone which were 27.7% viable. A similar pattern was seen in C3 cells which at 24 hours, those stimulated with BCR alone had 38.3% viability but those costimulated with NGFR.LMP1 and BCR were 27.1% viable but at 48 hours, viability of BCR-stimulated cells was 23.6% while those stimulated

with NGFR.LMP1 as well were 81.9% viable. Additionally, there is a trend of increased viability with CD40 and BCR costimulation in both cell lines at both time points. A4 cells at 24 h stimulated with BCR alone were 37.3% viable compared with cells stimulated with both BCR and CD40 which were 67.2% viable. C3 cells at 24 h stimulated with BCR alone were 38.3% viable but those stimulated with CD40 and BCR were 64.9% viable. At 48 h, A4 cells stimulated with BCR alone were 27.7% viable but those stimulated with CD40 and BCR were 60.7% viable. In C3 cells at 48 h, cells stimulated with BCR alone were 23.6% viable and those with both CD40 and BCR stimulation were 76.3% viable. These data corroborate CD40's ability to rescue cells from AICD. There is evidence that both CD40 and NGFR.LMP1 costimulation with BCR can provide some degree of rescue from AICD but due to the lack of applicable trials (those in which BCR stimulation alone induced >50% change in viability) none of these data are significant (Figure 7).

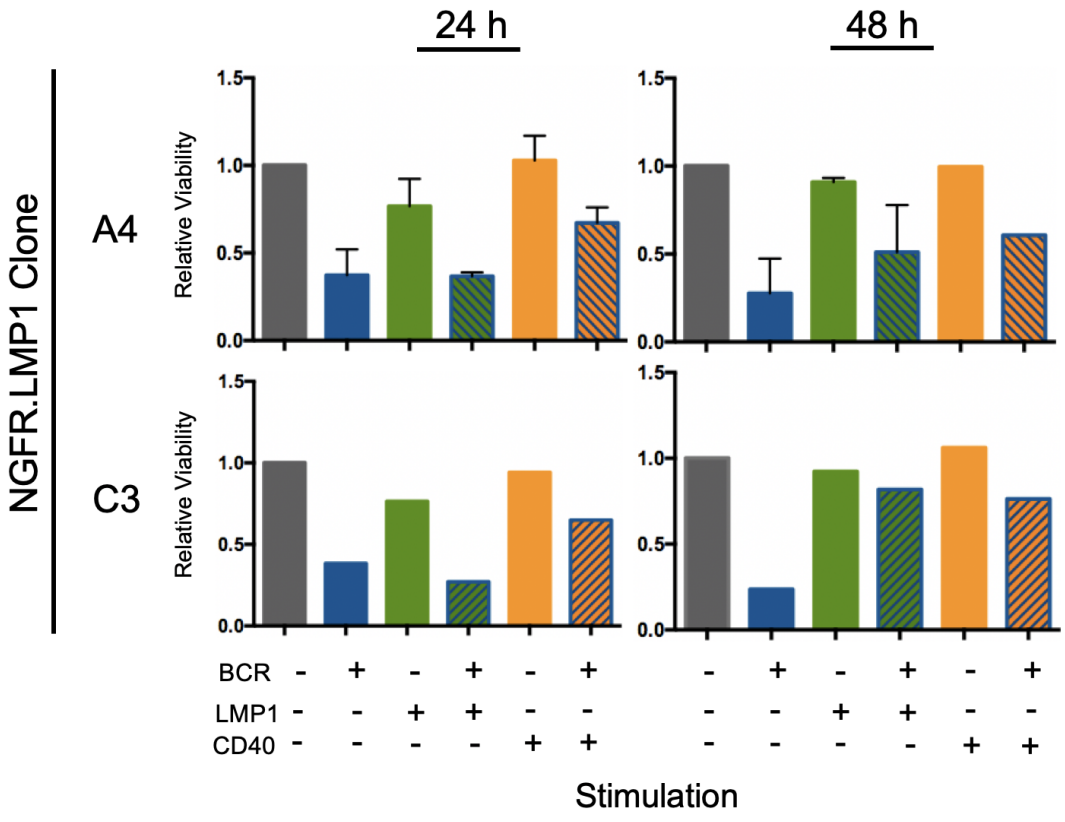

Figure 7. LMP1 and CD40 potentially rescue cells from AICD based on relative viability. After stimulation with anti-IgM alone or anti-IgM with CD40L or NGFR.LMP1 crosslinking, cell viability was measured via flow cytometry with cell viability stain 7-AAD. Populations were gated to exclude debris present in the samples and the percentage of viable cells was determined by percentage cells not stained with 7-AAD. Values were normalized to unstimulated samples.

Changes in ICAM expression do not correlate with cell viability

As an attempt to understand why we were not seeing the expected rescue effect, we assessed whether signal strength through NGFR.LMP1 (measured by ICAM fold change expression) could be correlated with one of our measures of assessing the rescue effect, here, cell viability. If there was a positive correlation between signal strength and viability, it may suggest that the second-signal stimulations were not strong enough for the full rescue effect to be seen in the context of the strength of the BCR stimulation. Fold change in ICAM expression was compared with percent viable cells and it was determined that there is no apparent correlation between ICAM expression and cell viability in cells stimulated by BCR alone, NGFR.LMP1 alone, or BCR + NGFR.LMP1 together (Figure 8). There also does not appear to be a consistent trend of magnitude or direction of changes in ICAM upregulation following stimulation with NGFR.LMP1 alone or with BCR+NGFR.LMP1 but ICAM is consistently downregulated in cells stimulated by the BCR alone. These data do not indicate a correlation between signal strength, measured by changes in ICAM expression, and cell viability.

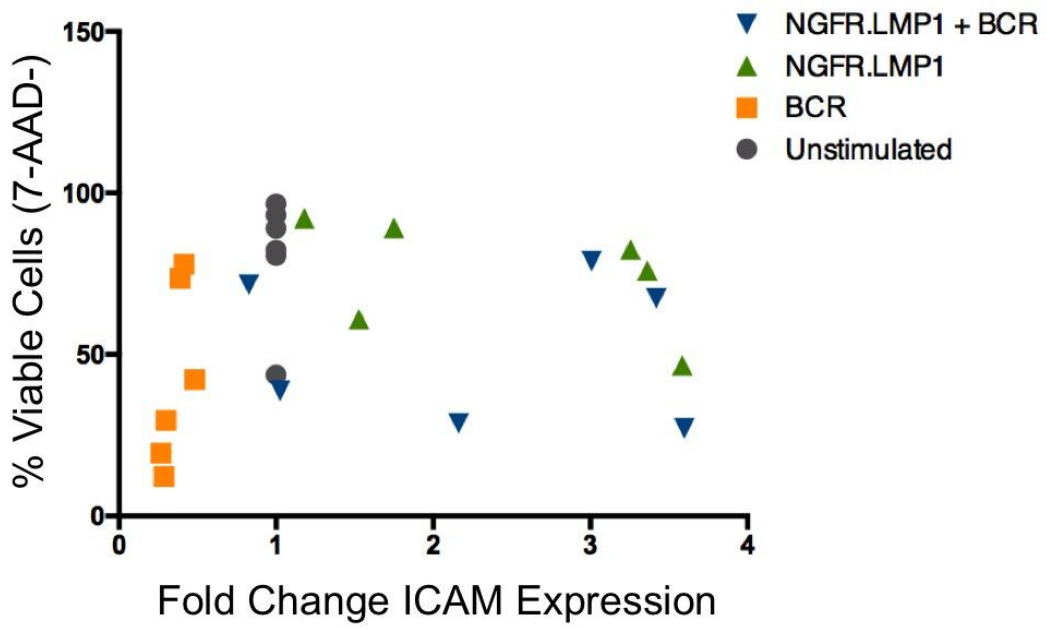

Figure 8. Increased ICAM expression does not correlate to increased cell viability. Ramos NGFR.LMP1 cells were stimulated for 24 or 48 h before collection for staining with PE ICAM antibody stain. Fold changes in ICAM expression for each trial were normalized within each experiment to unstimulated cells (grey circles). Cells were stimulated with F(ab')2 anti-human IgM + IgG alone (orange squares), mouse anti-human NGFR with goat anti-mouse cross-linking antibody alone (green triangles), or both anti-IgM and anti-NGFR with crosslinker (blue triangles). Fold change in ICAM expression was calculated from the Median Fluorescence Index (MFI) of PE ICAM fluorescence.

Part II: Transfection Optimization and Transfection of Ly49G.LMP2a Plasmid

Zeocin is the appropriate selection drug for the Ly49G.LMP2a plasmid

To investigate the role of LMP2a in the survival of cells infected by EBV, we sought to create a chimeric LMP2a protein in which signaling could be controlled by addition of exogenous cross-linking antibody. The chimeric LMP2a molecule consists of the external and transmembrane domains of the natural killer cell receptor Ly49G and the cytosolic domain of LMP2a. It does not contain the LMP2a transmembrane clustering domain, inhibiting the spontaneous aggregation and constitutive signaling seen in native LMP2a. Aggregation, and therefore signaling, can be induced by the addition of anti-Ly49G antibodies to cell culture media (Figure 9).

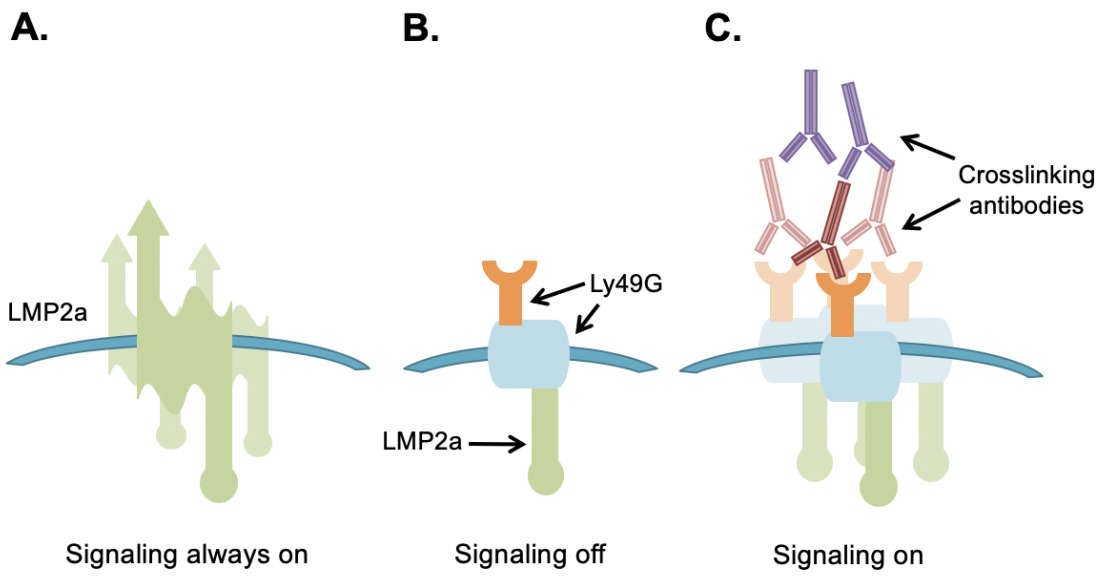

Figure 9. Native and chimeric LMP2a proteins. a) When expressed in B cells, LMP2a clusters on the cell membrane triggering constitutive signaling; this process disrupts normal inactive B cell signaling pathways and mimics activated BCR signaling. b) The chimeric Ly49G.LMP2a is comprised of the extracellular and transmembrane portions of Ly49G and the cytosolic portion of LMP2a. It does not contain the LMP2a transmembrane clustering domains and thus does not signal constitutively. Signaling can be triggered by adding antibody against Ly49G to cell media. c) When mouse anti-Ly49G antibody is introduced followed by anti-mouse cross-linker antibody, the Ly49G.LMP2a protein clusters and signals (c) as native LMP2a would signal in latent EBV-infected B cells.

To develop LCLs that express the construct, the proper selection conditions for LCLs expressing the plasmids were assessed. Toxicities of two antibiotics, hygromycin and Zeocin, were assessed in two EBV$^-$ Burkitt lymphoma cell lines, Ramos and BL41. Initially, ranges of drug concentration from 25-400 µg/mL for both drugs were tested to determine the IC50 for both drugs in each cell line. In BL41 cells, the IC_{50} values for zeocin and hygromycin were ~200 µg/mL and between 200-400 µg/mL respectively, at 72 hours. In Ramos cells, the IC50 values for zeocin and hygromycin were both between 200-400 µg/mL (Figure 10). From this initial experiment, we determined zeocin to have a lower IC_{50} allowing for lower concentrations of drug to be used, making it a better selecting agent. As the pcDNA3.1 (+) expression vector, which contains a G418 resistance gene, has been previously used to express the NGFR.LMP1 construct in Ramos and

BL41 cells, a similar plasmid containing a zeocin resistance gene, pcDNA3.1 (+) Zeo, was selected as the expression vector for the Ly49G.LMP2a construct.

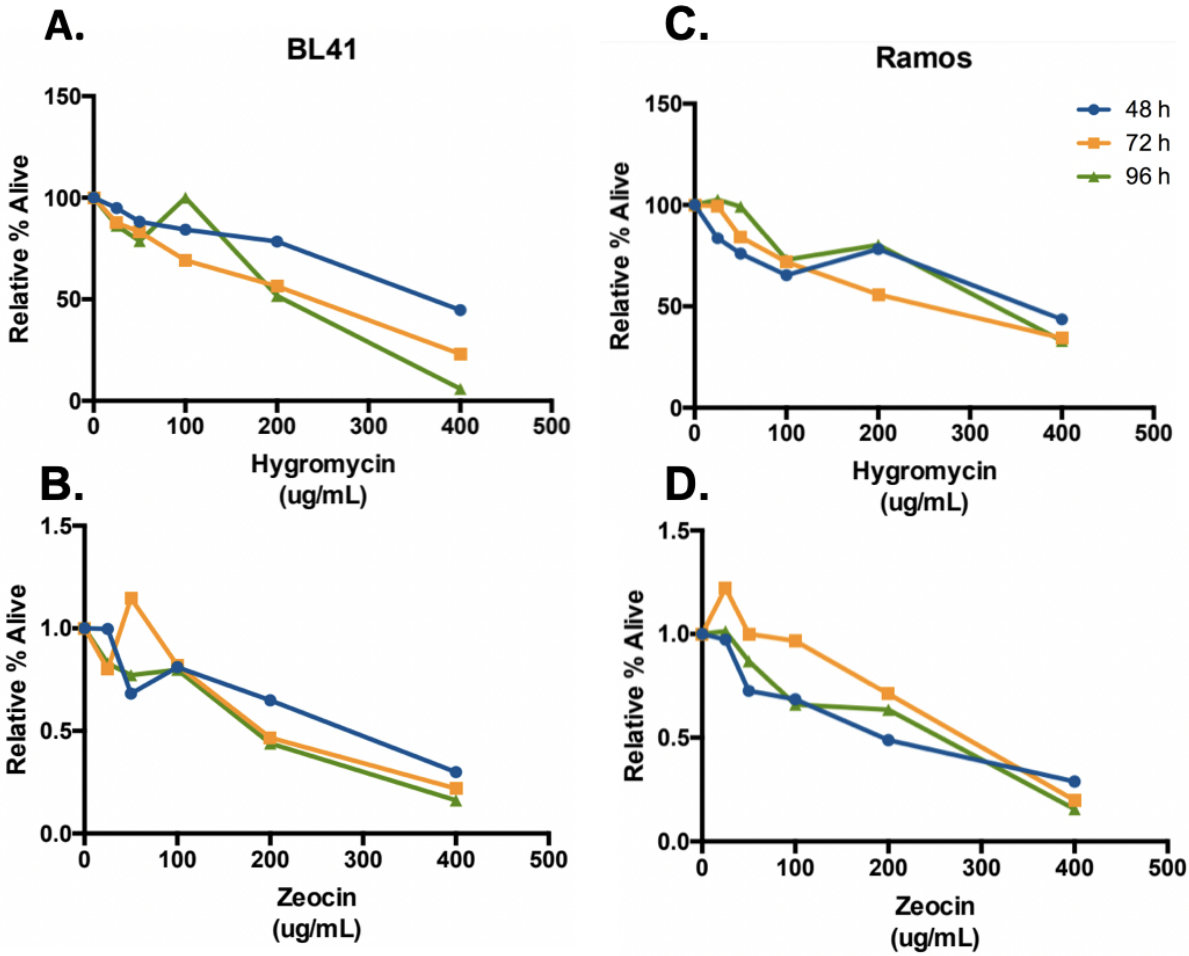

Figure 10. Zeocin can be used in selection at lower concentrations than hygromycin. Cells were grown in media containing 0-400 µg/mL with two-fold serial dilution of zeocin or hygromycin for 48, 72, and 96 hours. At 48 hours, cells were given an additional 500 µL of cRPMI containing the appropriate concentration of selection drug. At given time points, concentrations of living cells were determined using Trypan blue exclusion. Concentrations were normalized to untreated cells to determine relative % alive. N = 1.

The appropriate zeocin selection concentrations for Ramos and BL41 are 337.5 µg/mL and 112.5 µg/mL, respectively

After determining a range of potential selection concentrations, we performed a secondary kill curve with a narrowed range of concentrations of Zeocin only (Figure 11). From this experiment, we determined the IC50 of Zeocin for Ramos cells to be approximately 200 µg/mL and 75 µg/mL for BL41 cells. In order to ensure a strong selection for the plasmid construct, we chose to use higher concentrations of 450 µg/mL and 150 µg/mL for each cell line, respectively. These concentrations were used in initial attempts to select pcDNA3.1 (+) Zeo Ly49G.LMP2a containing cells following transfection. Ultimately, these concentrations were determined to be too high and following attempts used concentrations of 337.5 µg/mL and 112.5 µg/mL for Ramos and BL41 cells, respectively.

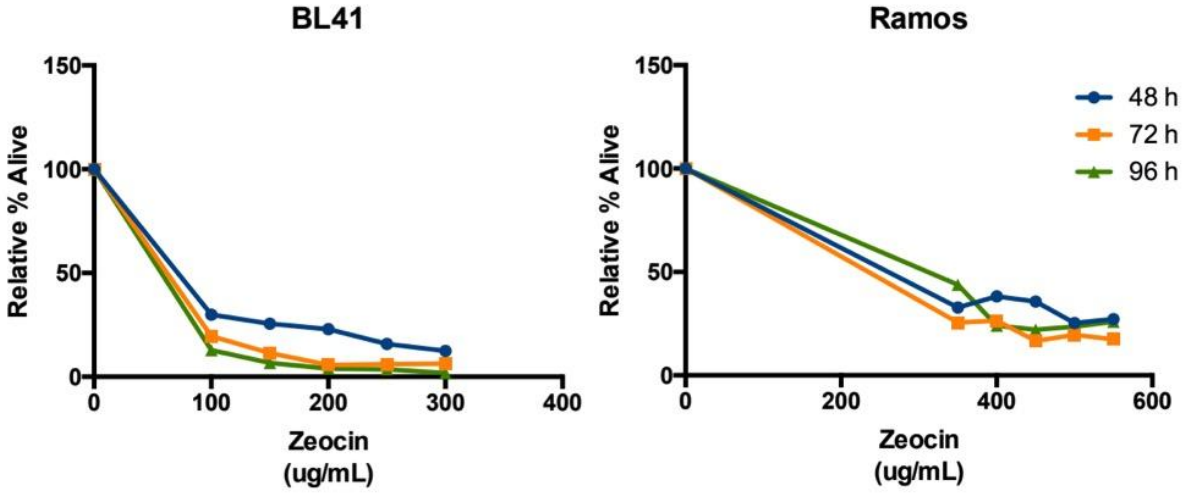

Figure 11. Optimal zeocin concentrations for selection are 337.5 and 112.5 µg/mL for Ramos and BL41, respectively. Kill curves were performed on both (a) Ramos and (b) BL41 Burkitt's Lymphoma B cell lines. Cells were cultured in 2 mL of varying concentrations (0, 100, 150, 200, 250, and 300 µg/mL for BL41, 0, 350, 400, 450, 500, and 550 µg/mL for Ramos) of Zeocin as indicated above. The number of live cells in each samples were counted at t = 48, 72, and 96 hours on a hemocytometer by Trypan blue exclusion. These counts were normalized to untreated samples at the same time points to determine the relative % alive. N = 1.

Successful construction of the pcDNA3.1 (+) Zeo Ly49G.LMP2a and pcDNA3.1 (+) Ly49G.LMP2a plasmids

The Ly49G.LMP2a construct was synthesized into the bacterial expression vector pUCIDT Kan. Both the expression vector and the construct vector (pcDNA3.1 (+) Zeo) containing the insert underwent a restriction enzyme digestion and purification by gel electrophoresis resulting in a 5 kb band containing the expression vector and two bands containing the construct vector (3.4 kb) and the Ly49G.LMP2a insert (~1.0 kb) (Figure 12).

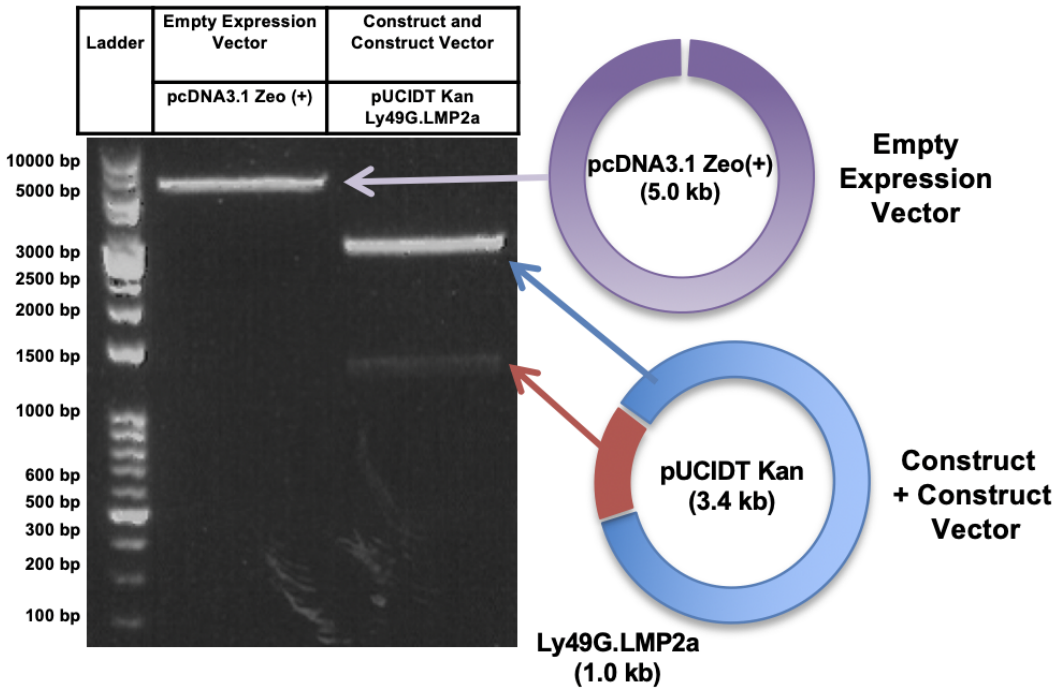

Figure 12. Gel purification of pcDNA3.1 (+) Zeo expression vector and pUCIDT Ly49G.LMP2a vector prior to ligation of final construct expression vector. Lane 1 (left) contains pcDNA3.1 Zeo (+) digested using Kpn I and Xho I restriction enzymes. Lane 2 (right) contains the pcDNA3.1 Zeo (+) Ly49G.LMP2a plasmid digested with *KpnI* and *XhoI*. Gels were run at 100V for 45 minutes on a 1% w/v agarose gel with GelRed DNA stain. (a) the results of the pre-purification RE digest (b) schematic diagrams of the empty expression vector (pcDNA3.1 Zeo(+)) and the initial construct plasmid synthesized by IDT.

The linearized expression vector and the insert were ligated to form the finished expression plasmid and were transformed into competent *E. coli*. 10 colonies were selected at

random for DNA isolation to confirm presence of the chimeric insert. Gel electrophoresis purification of restriction digested DNA from each of the 10 colonies resulted in a band of 1.0 kb and another of 5.0 kb, indicating the presence of Ly49G.LMP2a insert (Figure 13).

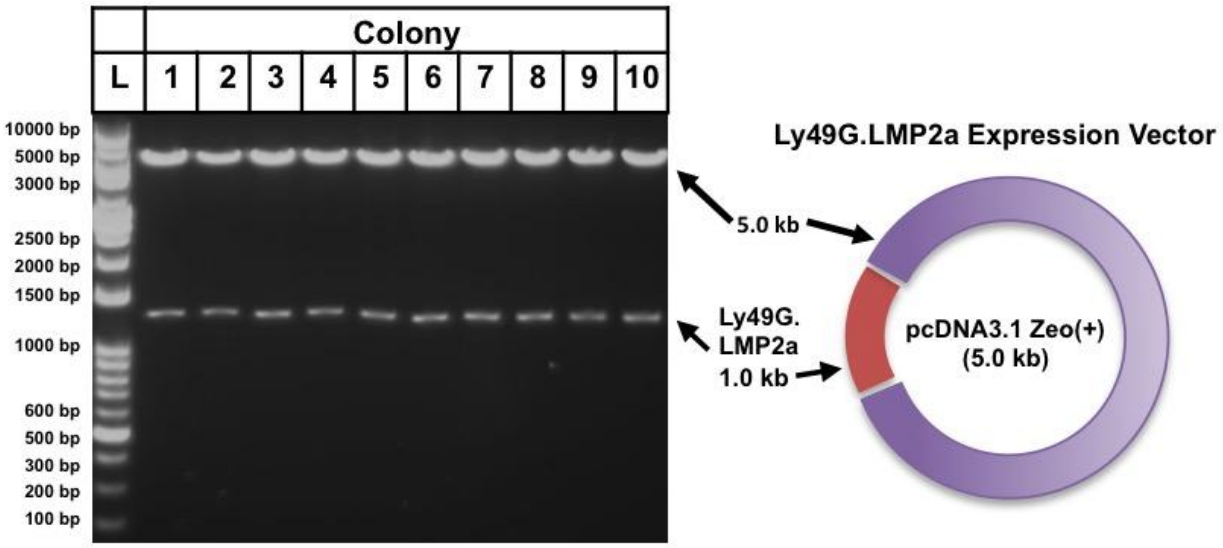

Figure 13. Confirming Construction of the Expression Vector pcDNA3.1 Zeo (+) Ly49G.LMP2a by Restriction Enzyme Digest. 10 colonies of *E. coli* transformed with the pcDNA3.1 Zeo (+) Ly49G.LMP2a plasmid were selected randomly from an LB ampicillin selection plate, inoculated for ~16 hours at 37C with shaking in 1x LB ampicillin, and plasmid DNA was isolated using Qiagen Plasmid Mini-Prep kit. DNA from each of the 10 colonies was then digested using *KpnI* and *XhoI* restriction enzymes and the products of each digest were run on 1% w/v agarose stained with GelRed for 45 minutes at 100V. L = Versa 1kb ladder.

DNA from the same 10 colonies was sequenced with Sanger technology and analyzed to identify any transformants that contained mutations. Of the 5 colonies sequenced, three contained a mutation that caused a premature stop codon and only 1 contained an insert with a sequence identical to that of the reference sequence used to generate the insert (Figure 14).

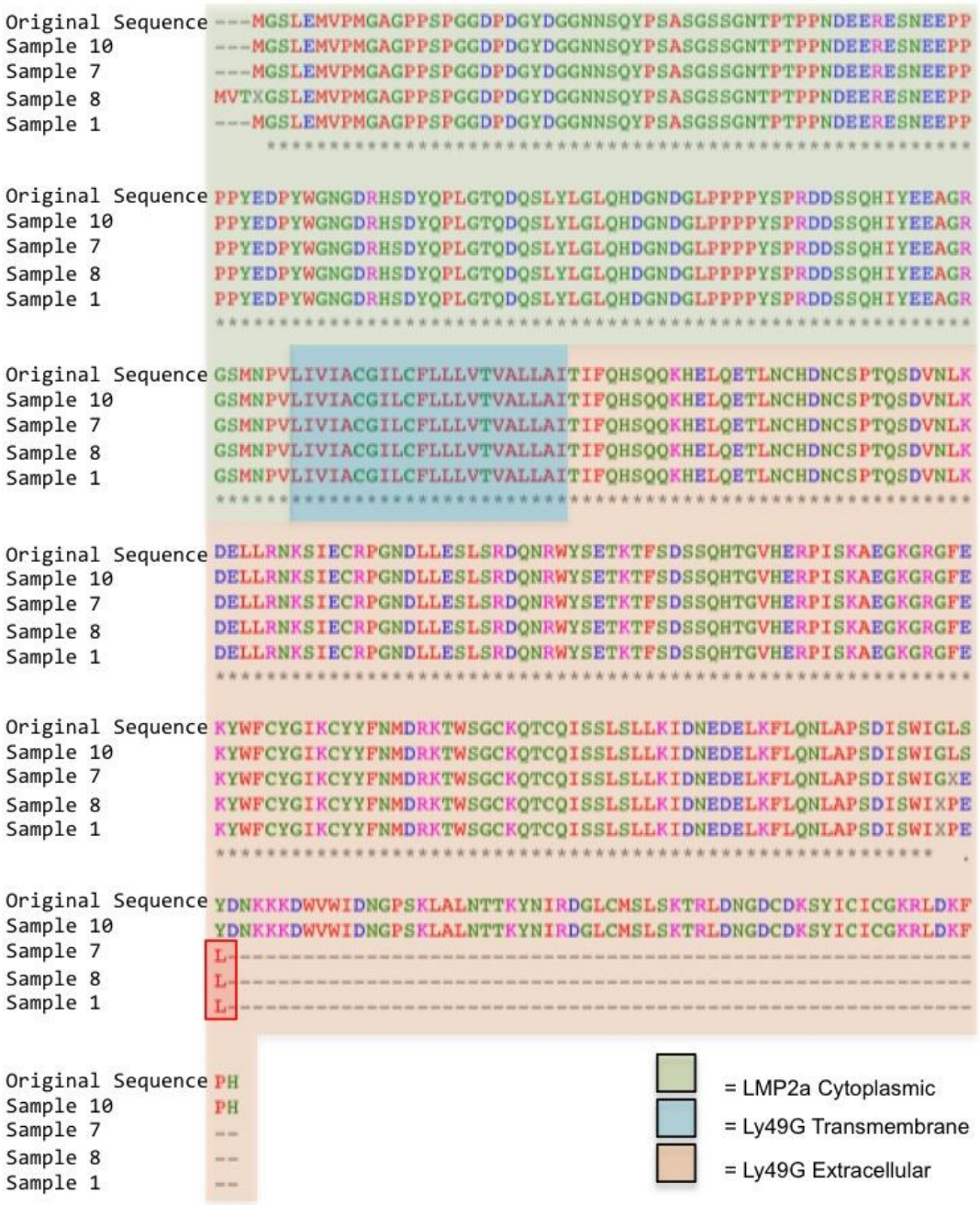

Figure 14. Confirming Construction of the Expression Vector pcDNA3.1 Zeo (+) Ly49G.LMP2a by Sanger Sequencing. 5 colonies were chosen at random to be sequenced using Sanger sequencing. Each sequence was analyzed using Sequencher sequence-alignment tools. Analysis revealed that three of the five colonies selected contained a mutation that induced a premature stop codon. One sample, sample 10, had the appropriate sequence. Areas highlighted in green indicate the cytoplasmic LMP2a portion of the protein sequence, areas highlighted in blue indicate the transmembrane Ly49G sequence, and areas highlighted in orange indicate the extracellular Ly49G sequence. Incidence of the premature stop codon is highlighted in red.

The plasmid with the correct insert was then transfected into Ramos and BL41 cell lines under the optimized conditions described below. The initial transfection did not result in growth of clones and so a second transfection was performed. This transfection resulted in two colonies of BL41 cells that had small numbers of cells expressing Ly49G as determined by fluorescent antibody staining (Figure 15). Attempts to further expand these cell lines resulted in their loss. Subsequent attempts to isolate colonies expressing the pcDNA3.1 (+) Zeo Ly49G.LMP2a construct were unsuccessful and a new plasmid carrying the insert was synthesized in the pcDNA3.1 (+) backbone which has been effective in the construction and expression of the NGFR.LMP1 construct.

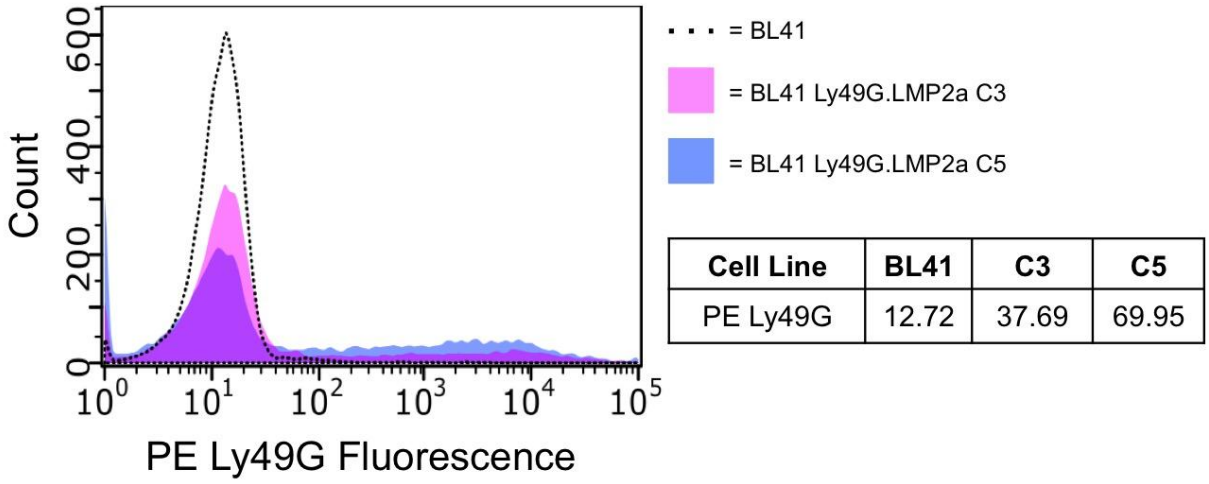

Cell Line	BL41	C3	C5
PE Ly49G	12.72	37.69	69.95

Figure 15. Two colonies of BL41 transfected with the Ly49G.LMP2a plasmid have some expression of Ly49G.LMP2a. Colonies of cells were collected from 96-well selection plates once cells were visible in the wells. Cells were then removed from selection media, resuspended in FACS buffer, and stained with anti-Ly49G PE antibody and analyzed with flow cytometry. The mean PE fluorescence for each sample was determined (PE Ly49G) and compared to BL41 cells not transfected with the pcDNA3.1(+) Zeo Ly49G.LMP2a plasmid.

A similar process to the above was followed to create pcDNA3.1 (+) Ly49G.LMP2a and the finished plasmid was transformed into competent *E. coli*. Plasmid DNA was then isolated, digested, and separated with gel electrophoresis. Bands containing fragments of the appropriate sizes for the insert (1.0 kb) and the expression vector (5.0 kb) were present in all colonies sampled, (Figure 16) confirming the presence of the insert. Isolated DNA was then sequenced

using Sanger sequencing (data not shown) and it was determined that of the five colonies sequenced, there were no apparent mutations present indicating that the pcDNA3.1 (+) Ly49G.LMP2a plasmid can be transfected into cells. Currently, no such attempt has been made due to lack of availability of an electroporation system at Stanford Medical School facilities.

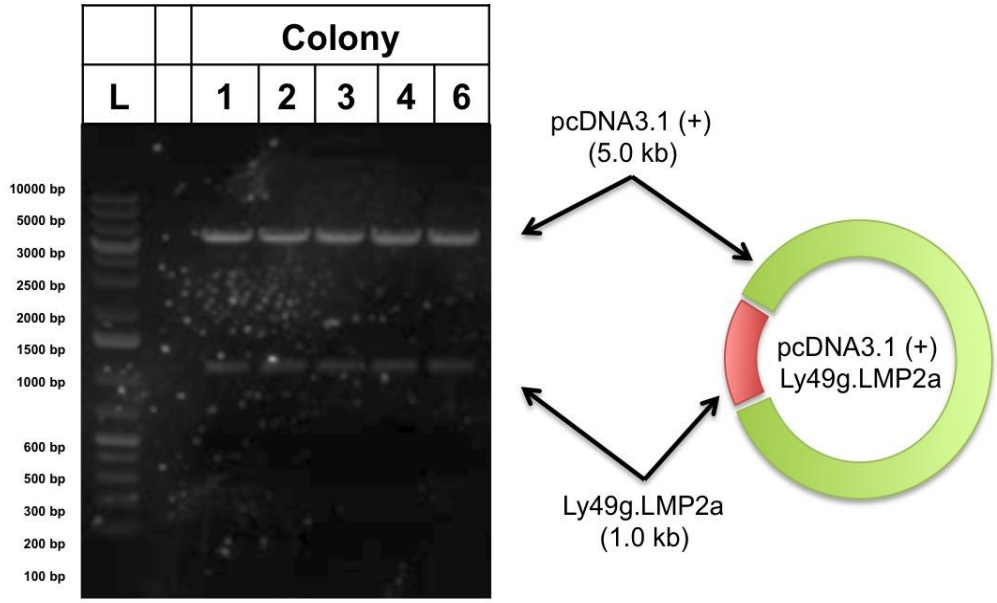

Figure 16. Confirming construction of the expression vector pcDNA3.1 (+) Ly49G.LMP2a by restriction enzyme digest. 6 colonies of *E. coli* transformed with the pcDNA3.1 (+) Ly49G.LMP2a plasmid were selected randomly from an LB ampicillin agar selection plate, inoculated for ~16 hours at 37C with shaking in 1X LB ampicillin. Plasmid DNA was successfully isolated from 5 of the 6 colonies using Qiagen Plasmid Mini-Prep kit. DNA from each of the 5 colonies was then digested using *KpnI* and *XhoI* restriction enzymes and the products of each digest were run on 1% w/v agarose with GelRed DNA stain for 45 minutes at 100V. Products of the digest were visualized by UV photodocumentation. L = GoldBio 1kb ladder.

Optimal transfection conditions for Ramos and BL41 cells are 1 shock at 1000V with 1 µg DNA/ 1 x 10^6 cells

To maximize transfection efficiency of the pcDNA3.1 (+) Zeo Ly49G.LMP2a plasmid, we optimized transfection conditions in both Ramos and BL41 cells using a GFP expression plasmid. Transfection efficiency and post-transfection viability were assessed by flow cytometry for GFP-expression and staining for viability with 7-AAD. We utilized the MicroPulser electroporation

system for our transfections and optimized the following parameters: shock intensity / voltage, number of pulses, and amount of DNA.

Cells were shocked at 750V, 1000V, and 1250V a single time. Samples shocked with 750V achieved a maximum % GFP^+, viable cells with 15.79% and 16.45% for BL41 and Ramos cells respectively. Cells shocked at 1000V achieved a maximum % GFP^+, viable cells with 26.57% and 28.54% for BL41 and Ramos respectively. Shocking cells at 1250V resulted in the MicroPulser delivering an “arc” error and maximum transfection rates of 4.75% and 0.99% for BL41 and Ramos cells respectively. A slight decrease in cell viability was observed in samples shocked at 1000V compared to 750V. For BL41 and Ramos cells shocked at 750V, the maximum percent non-viable (GFP^-, 7-AAD^+) was 2.65% and 2.12%, respectively. BL41 shocked at 1000V had a maximum loss of viability of 1.59% while Ramos had a slightly greater loss at 3.82%. 1000V was determined to be the optimal intensity as it did not result in substantially more non-viable cells than shocking at 750V but yielded higher levels of transfected cells (Figure 17a, panels 1 and 2). 1250V was not optimal because the conductivity of the serum-free media in which the transfections took place was too high for a shock of that intensity (Figure 17a, panel 3).

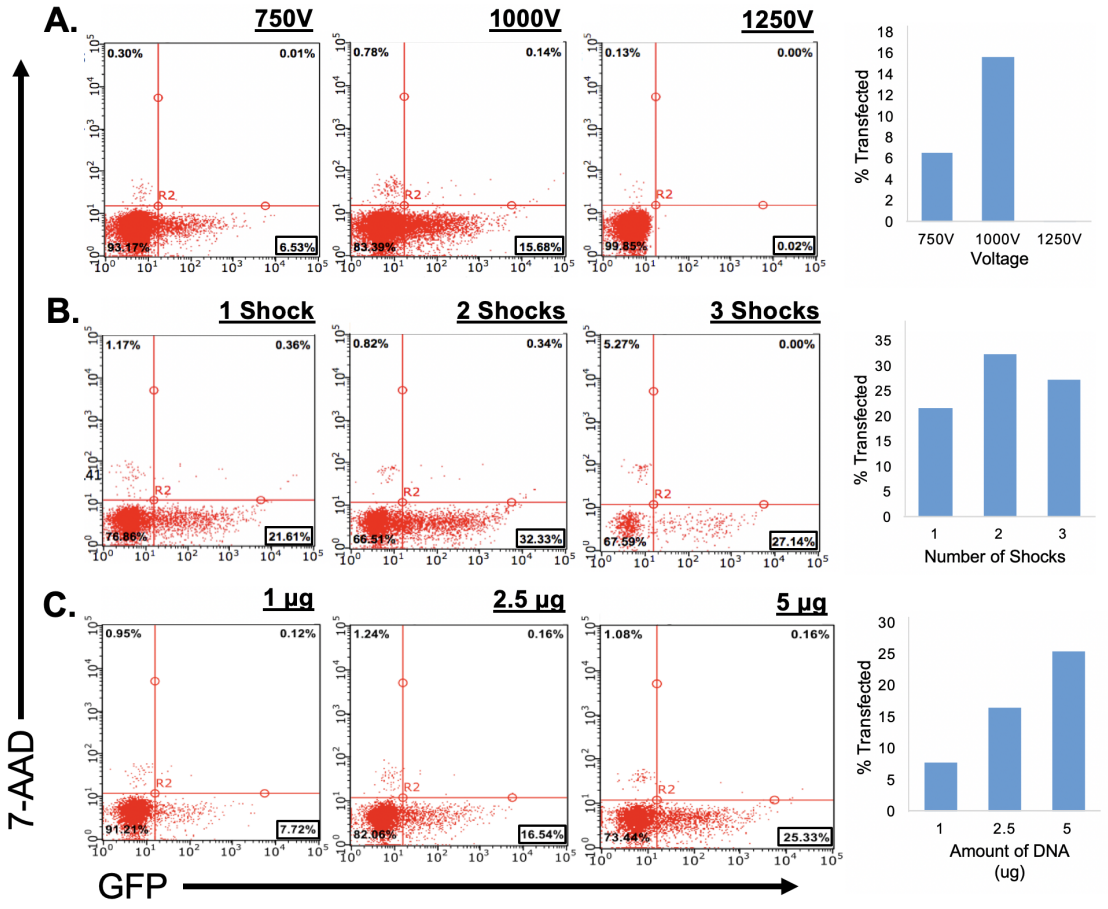

Figure 17. Optimal transfection conditions are 1 shock at 1000V with 5 µg DNA/sample. Transfections were performed via electroporation (BioRad MicroPulser Electroporator) and GFP-expression plasmid (pMaxGFP). Samples were stained with 7-AAD viability stain and analyzed flow cytometry for the percent 7-AAD$^-$GFP$^+$ cells, which reflects the percent of viable cells that were successfully transfected with the pMaxGFP plasmid. In each trial, 5x10^6 cells were transfected in 200-220 µL of serum-free RPMI media. (a) Cells were transfected with 5 µg DNA at 750V, 1000V, and 1250V respectively. (b) Cells were transfected with 5 µg DNA at 1000V 1, 2, and 3 times respectively. (c) Cells were transfected with one shock at 1000V with 1, 2.5, and 5 µg DNA respectively.

The effect of the number of shocks given to each sample was also determined. Cells were given 1, 2, or 3 shocks at 1000V. Maximum transfection efficiency for Ramos and BL41 cells with 1 shock was 18.55% and 21.61% respectively. Viability after 1 shock was high with 0.66% and 1.17% non-viable for Ramos and BL41. Shocking cells twice resulted in higher transfection efficiency with 20.99% and 32.33% GFP$^+$ cells for Ramos and BL41. Viability was slightly decreased in Ramos cells, with 2.50% non-viable cells, and slightly increased in BL41 with 0.82%

non-viable. However, cell concentrations were decreased, indicating more cells had died in the transfection process. Shocking cells three times resulted in 20.73% transfected Ramos cells and 27.14% of BL41 cells transfected but 4.63% and 5.72% of cells were non-viable in each cell line respectively and cell concentrations were greatly reduced. Representative data from BL41 are shown in Figure 17b. A single shock was determined to be the most effective as it yields high levels of transfection without a consequent loss in viability or proliferation.

The effect of the amount of plasmid DNA added to each sample (5×10^6 cells) was also tested and it was found that transfection efficiency increased to the amount of DNA added (Figure 17c) with 15 µg/ sample generating the highest proportion of transfected cells (18.52%) in Ramos and 10 µg/sample (28.60%) in BL41. In line with this observation, transfecting cells with 1 µg/sample resulted in 2.19% transfection for Ramos cells and 7.72% for BL41. However, transfecting cells with 5 µg DNA/sample resulted in 15.04% transfected in Ramos and 24.34% in BL41, indicating that increasing the concentration of DNA above 5 µg/sample may not provide added benefit. Viability and cell concentration were not substantially affected by variations in DNA concentration used.

Taken together, the optimal transfection conditions for both Ramos and BL41 cells are a single shock at 1000V with 5 µg DNA/5×10^6 cells. Although increasing the amount of DNA can increase transfection efficiency, the efficiency achieved with a lower concentration of DNA is satisfactory. Decreasing shock intensity increases viability but the improvements to viability are not substantial enough to warrant the decreases in transfection efficiency. Although shocking the cells more than once increases transfection efficiency, the increase is not substantial enough to warrant the loss in cell concentration.

Discussion

Part I: Effects of LMP1 as a Second Signal on Cell Proliferation and Viability in B cells

We sought to determine the ability of both CD40 and LMP1 to rescue cells from AICD following stimulation via the BCR. We found that BCR signaling alone had the ability to cause large losses in cell viability and proliferation but this effect was not seen in each of the five trials performed. In trials in which AICD was triggered by BCR stimulation alone, varying degrees of rescue were provided by both CD40 and NGFR.LMP1 signaling but due to the number of trials excluded due to the lack of effect seen from BCR stimulation alone, these data lacked overarching significance.

Because of the lack of statistical significance, these results somewhat contradict research in HEL-specific MD4 murine B cells[8] indicating that CD40 signaling is able to provide a rescue effect from BCR-induced AICD, we were unable to significantly replicate these findings in human LCL cells, although there did appear to be a trend toward increased viability and cell proliferation with costimulation of CD40 and BCR. Differences in this effect could potentially be explained by biological differences between transformed cell lines and non-transformed naive cells. Similarly, the inconsistency of rescue provided by LMP1 signaling could be explained by differences in signal transduction between transformed and untransformed cells. It is also possible that in both cases, the concentrations of stimulations are not aligned in such a way for rescue effects to be readily detectable. If BCR stimulation is too strong, the resultant drop in proliferation and viability could potentially be masking rescue effects of CD40 and LMP1. Following this line of reasoning, we found that level of ICAM upregulation does not correlate to cell viability under any stimulation condition. A correlation might have provided further evidence for the rescue trend that was found.

In both CD40 and NGFR.LMP1 stimulations alone, there was a consistent trend of mild cytotoxicity of these stimulations in comparison to untreated cells. In fact, although LMP1 is canonically understood to drive cellular proliferation in EBV-infected cells, there is some evidence that high levels of LMP1 expression can lead to Fas overexpression which overrides the

proliferative effects of LMP1-driven NF-κB signaling resulting in apoptosis[19]. Similarly, although CD40 signaling is known to promote cell survival, ligation of CD40 with its ligand, through crosslinking, or T cell interaction can promote the expression of Apo-1/Fas antigen which can then trigger Fas-mediated apoptosis through anti-Apo-1/Fas antibody[20] indicating the existence of a balance between cell-survival and apoptosis during B cell activation.

Functionality of the NGFR.LMP1 construct in this and previous research has been indicated by upregulation of ICAM which is also upregulated by stimulation through CD40, indicative of the overlap of signaling pathways shared by the two molecules. Although LMP1 increases expression of ICAM in Ramos and BL41 cell lines, effects of LMP1 signaling have been demonstrated to be more heterogeneous than CD40 signaling in LCLs with cell line specific patterns of surface marker upregulation[21]. CD40's effects are more concise and primarily involve upregulation of ICAM and CD18, leading to activation of the CD18-dependent cellular adhesion system[22] in the native context. There may then be a need for assessment of the metrics used to determine functionality of the NGFR.LMP1 construct in light of cell line specific differences in signal effects of LMP1 and the potential for inequivalent measures of signaling between CD40 and LMP1. A marker for signaling of one protein may not correlate in an equivalent fashion to signaling in the other.

Effects of LMP1 crosslinking on metabolism are potentially demonstrated by significant increases in MitoTracker Green (MTG) staining. MTG, although developed as a means of measuring mitochondrial mass in cells, has also come into usage as a way to quantify mitochondrial injury[18] as dysfunctional mitochondria stain more heavily with MTG than homeostatic mitochondria. Literature concerning the use of MTG as a reliable means of measuring mitochondrial mass in a manner independent of other factors like mitochondrial membrane potential and oxidative stress is inconclusive. Keij et al.[23] found that MTG staining was sensitive to the addition of drugs that alter mitochondrial membrane potential while Pendergrass et al.[24] found that it was not susceptible to influence from either changes in mitochondrial

membrane potential or oxidative stress. In order to conclusively discern the meaning of changes in MTG staining, another measure of either mitochondrial function or mass is required. If it can be confirmed that MTG staining does correlate with mitochondrial mass in these studies, further investigation into the etiology of changes is required. Possible avenues of investigation include determination of the biologic pathways leading to changes in mitochondria and effects on signaling, especially those related to ROS production.

Although the ability of LMP1 and CD40 signaling to rescue B cells from post-BCR stimulation AICD remains inconsistent, there are trends that suggest that with further testing and slight alterations in methods of assessment a “rescue effect” may be observed. Further efforts to successfully develop a functional and inducible LMP2a will continue the the ultimate goal of creating a system of testing effects of both LMP1 and LMP2a in a single cell line.

Part II: Transfection Optimization and Transfection of Ly49G.LMP2a Plasmid

The ultimate goal of the development of the Ly49G.LMP2a plasmid construct is to co-transfect cells with both Ly49G.LMP2a and NGFR.LMP1. By doing so, signaling from both of these normally constitutively active proteins can be triggered in order to better understand the interplay and modulation these two viral proteins during latent infection. Part of this strategy was to have different selection markers on each construct plasmid in order to have the ability to perform a double selection on cells transfected with both plasmids, allowing for an expedited identification of clones expressing both constructs. After performing kill curves to determine the appropriate drug and concentration for selection of the Ly49G.LMP2a construct, transfections and subsequent selection protocols were followed with limited success. Initially, it was found that concentrations of 450 µg/mL and 150 µg/mL Zeocin for Ramos and BL41 cells, respectively, were too high as colonies isolated from these growth conditions did not test positive for Ly49G with staining for flow cytometry (data not shown). Following initial attempts, the selection concentrations were reduced to ¾ of their original values (337.5 µg/mL, 112.5 µg/mL) and the

transfection protocol was repeated resulting in two colonies with low numbers of cells staining positive for Ly49G.

Following initial detection of these colonies, no subsequent clones expressing the construct were detected, with observationally high levels of cellular debris and few cells present in isolated colonies which potentially indicates that the selection concentration is still too high and cells that were initially expressing the plasmid containing the Zeocin resistance gene were unable to cope with high levels of drug. The second possibility is that there is something about the construct or plasmid backbone that is incompatible with cell viability. Assessing whether the pcDNA3.1 (+) Zeo expression plasmid is a simpler fix than designing a novel LMP2a construct so the next step was to place the existing Ly49G.LMP2a sequence into a plasmid known to work in Ramos and BL41 cells, pcDNA3.1 (+), which contains a resistance gene for G418. Sequencing of the resulting pcDNA3.1 (+) Ly49G.LMP2a plasmid indicated that the plasmid had been inserted in the correct orientation with the correct sequence for all five colonies sequenced. Available resources have not yet allowed for transfection attempts using the new plasmid but when possible, selection concentration of G418 used for the NGFR.LMP1 construct plasmid will be utilized.

In attempting to explain the inability to isolate cells that stably express the construct, it is also possible that there is something wrong with the Ly49G.LMP2a construct itself. As it is a chimeric protein generated, essentially, by cutting and pasting two unrelated sequences together, it seems possible that there is something about the resulting tertiary structure that is incompatible with protein processing machinery. As it is expressed under the highly active CMV promoter, high levels of the misfolded protein may be produced. If it is unable to be inserted into the cell membrane where it can function as intended, it may simply accumulate in the endoplasmic reticulum, triggering the unfolded protein response, eventually leading to apoptosis[25]. Instances in which Ly49G was detected at low levels indicate that this is not necessarily the case but further attempts at transfection and selection are required to rule this possibility out.

Acknowledgements

I would like to thank Dr. Olivia Hatton for her outstanding dedication and mentorship over the course of my career at Colorado College and for providing extensive opportunities to practice science and for creating a forgiving environment in which to learn. I would also like to thank Dr. Phoebe Lostroh for her guidance in writing this thesis and for being an amazing role model for women in STEM. Additionally, I would like to thank Drs. Sheri Martinez and Olivia Krams at Stanford Medical School for allowing me to experience a taste of research at a prestigious research institution and for being both welcoming and supportive. Thank you, also, to Dr. Sara Hanson and Dr. Jenn Garcia for contributing extensively to my education in Molecular Biology and for always offering support and understanding.

References

1. Green, M. & Michaels, M. G. Epstein-Barr Virus Infection and Posttransplant Lymphoproliferative Disorder. *American Journal of Transplantation* **13,**41–54 (2013).

2. Hassani, A., Corboy, J. R., Al-Salam, S. & Khan, G. Epstein-Barr virus is present in the brain of most cases of multiple sclerosis and may engage more than just B cells. *Plos One* **13,**(2018).

3. Kempkes, B. & Robertson, E. S. Epstein-Barr virus latency: current and future perspectives. *Current Opinion in Virology* **14,**138–144 (2015).

4. Ma, S.-D. *et al.* Latent Membrane Protein 1 (LMP1) and LMP2A Collaborate To Promote Epstein-Barr Virus-Induced B Cell Lymphomas in a Cord Blood-Humanized Mouse Model but Are Not Essential. *Journal of Virology* **91,** (2017).

5. Uchida, J. Mimicry of CD40 Signals by Epstein-Barr Virus LMP1 in B Lymphocyte Responses. *Science* **286,**300–303 (1999).

6. Rastelli, J. *et al.*LMP1 signaling can replace CD40 signaling in B cells in vivo and has unique features of inducing class-switch recombination to IgG1. *Blood* **111,**1448–1455 (2008).

7. Vrazo, A. C., Chauchard, M., Raab-Traub, N. & Longnecker, R. Epstein-Barr Virus LMP2A Reduces Hyperactivation Induced by LMP1 to Restore Normal B Cell Phenotype in Transgenic Mice. *PLoS Pathogens* **8,**(2012).

8. Engels, N. *et al.* Epstein-Barr virus LMP2A signaling in statu nascendi mimics a B cell antigen receptor-like activation signal. *Cell Communication and Signaling* **10,**9 (2012).

9. Caro-Maldonado, A. *et al.* Metabolic Reprogramming Is Required for Antibody Production That Is Suppressed in Anergic but Exaggerated in Chronically BAFF-Exposed B Cells. *The Journal of Immunology* **192,**3626–3636 (2014).

10. Boothby, M. & Rickert, R. C. Metabolic Regulation of the Immune Humoral Response. *Immunity* **46,**743–755 (2017).

11. Adams, W. C. *et al.* Anabolism-Associated Mitochondrial Stasis Driving Lymphocyte Differentiation over Self-Renewal. *Cell Reports* **17,**3142–3152 (2016).

12. Doughty, C. A. Antigen receptor-mediated changes in glucose metabolism in B lymphocytes: role of phosphatidylinositol 3-kinase signaling in the glycolytic control of growth. *Blood* **107,**4458–4465 (2006).

13. Mehta, M. M., Weinberg, S. E. & Chandel, N. S. Mitochondrial control of immunity: beyond ATP. *Nature Reviews Immunology* **17,**608–620 (2017).

14. Wheeler, M. L. & Defranco, A. L. Prolonged Production of Reactive Oxygen Species in Response to B Cell Receptor Stimulation Promotes B Cell Activation and Proliferation. *The Journal of Immunology* **189,**4405–4416 (2012).

15. Jang, K.-J. *et al.* Mitochondrial function provides instructive signals for activation-induced B-cell fates. *Nature Communications* **6,**(2015).

16. Jellusova, J. *et al.* Gsk3 is a metabolic checkpoint regulator in B cells. *Nature Immunology* **18,**303–312 (2017).

17. Phan, T. G. & Tangye, S. G. B cells race the clock to get a second wind. *Nature Immunology* **19,**791–793 (2018).

18. Akkaya, M. *et al.* Second signals rescue B cells from activation-induced mitochondrial dysfunction and death. *Nature Immunology* **19,**871–884 (2018).

19. Clorennec, C. L. *et al.* Molecular Basis of Cytotoxicity of Epstein-Barr Virus (EBV) Latent Membrane Protein 1 (LMP1) in EBV Latency III B Cells: LMP1 Induces Type II Ligand-Independent Autoactivation of CD95/Fas with Caspase 8-Mediated Apoptosis. *Journal of Virology* **82,**6721–6733 (2008).

20. Schattner, E. J. CD40 ligation induces Apo-1/Fas expression on human B lymphocytes and facilitates apoptosis through the Apo-1/Fas pathway. *Journal of Experimental Medicine* **182,**1557–1565 (1995).

21. Wang, F., Tsang, S.-F. & Kurilla, M. G. Epstein-Barr Virus Nuclear Antigen 2 Transactivates Latent Membrane Protein LMP1. *Journal of Virology* **64,**3407–3416 (1990).

22. Barrett, T. B., Shu, G. & Clark, E. A. CD40 signaling activates CD11a/CD18 (LFA-1)-mediated adhesion in B cells. *Journal of Immunology* **146,**1722–1729 (1991).

23. Keij, J. F., Bell-Prince, C. & Steinkamp, J. A. Staining of mitochondrial membranes with 10-nonyl acridine orange MitoFluor Green, and MitoTracker Green is affected by mitochondrial membrane potential altering drugs. *Cytometry* **39,**203–210 (2000).

24. Pendergrass, W., Wolf, N. & Poot, M. Efficacy of MitoTracker Green and CMXrosamine to measure changes in mitochondrial membrane potentials in living cells and tissues. *Cytometry* **61A,**162–169 (2004).

25. Walter, P. & Ron, D. The Unfolded Protein Response: From Stress Pathway to Homeostatic Regulation. *Science* **334,**1081–1086 (2011).